Metal–Organic Frameworks

DOI: 10.1002/anie.200804853

A Luminescent Microporous Metal–Organic Framework for the Fast and Reversible Detection of High Explosives**

*Anjian Lan, Kunhao Li, Haohan Wu, David H. Olson, Thomas J. Emge, Woosoek Ki, Maochun Hong, and Jing Li**

Detection of high explosives is attracting increasing attention owing to homeland security, environmental and humanitarian implications.[1] 2,4-Dinitrotoluene (DNT), an inevitable byproduct in the manufacturing process of 2,4,6-trinitrotoluene (TNT), has a room-temperature vapor pressure about 20 times that of the latter. Therefore, the detection of nitroaromatic explosives is often achieved by detection of DNT. Conversely, plastic explosives often do not contain nitroaromatics, and their detection is consequently realized by detection of 2,3-dimethyl-2,3-dinitrobutane (DMNB, a taggant required by law in all commercial plastic explosives). In search of more convenient and cost-effective alternatives to the well-trained canines[2] or sophisticated analytical instruments,[3] new molecular, oligomeric, polymeric, and nanoscale materials that are capable of fast and reliable sensing of the above chemicals have recently been identified.[4–9] Fluorescence redox quenching is often the working mechanism within these systems.[4,5] Although extremely high sensitivity towards nitroaromatic explosives has been demonstrated, detection of DMNB remains a great challenge, largely owing to its unfavorable reduction potential (-1.7 V vs. SCE) and weak binding to the sensory materials, which arises from its three-dimensional molecular structure and lack of π–π interactions.[10]

Microporous metal–organic frameworks (MMOFs) are a new class of zeolite-like crystalline material, and have been shown by recent research to have great potential for a wide range of applications, such as molecular storage and separation, catalysis, and sensing.[11] A small number of MMOFs have been discovered which are luminescent in the solid state.[12] The combination of luminescence and accessible porosity within such materials imparts them with the capability of transducing the host–guest chemistry to detectable changes in their luminescence and makes them promising candidates for chemical sensing applications.[13] The work reported herein demonstrates, for the first time, that the highly luminescent microporous metal–organic framework $[Zn_2(bpdc)_2(bpee)]$ (bpdc = 4,4′-biphenyldicarboxylate; bpee = 1,2-bipyridylethene) is capable of very fast and fully reversible detection of both DNT and DMNB with unprecedented sensitivity.

Colorless block-shaped crystals of $[Zn_2(bpdc)_2(bpee)]\cdot 2\,DMF$ (**1**) were grown solvothermally. Study by single crystal X-ray diffraction disclosed a 3D framework structure in the monoclinic space group *C*2/*c*. The overall structure can be viewed as bpee ligands pillaring the undulating charge-neutral $[Zn_2(bpdc)_2]$ layers (Figure 1 a).

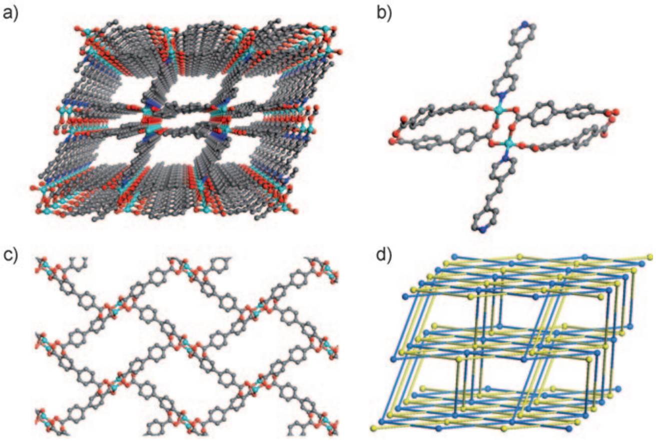

Figure 1. a) Perspective view of the 3D structure of **1**, showing the channels along the *b* axis (DMF molecules are removed for clarity); b) the eight-membered ring-type SBU and the coordination around Zn^{II}; c) a single 4^4 (brick-like) net (Zn turquoise; C gray; O red; N blue); d) simplified framework connectivity by linking the centroids of SBUs (spheres). Blue and yellow highlight the twofold interpenetration.

Two bidentate carboxylate groups from two centrosymmetrically related bpdc ligands coordinate to two Zn^{II} centers to form the $\{Zn_2(COO)_2^{2+}\}$ corrugated eight-membered ring-type secondary building unit (SBU; Figure 1 b). Two monodentate carboxylates from another pair of centrosymmetrically related bpdc ligands coordinate to the two Zn^{II} centers, balancing the charges on the SBU. Thus each SBU becomes a four-connecting node, which is linked by bpdc ligands to four other SBUs to form the two-dimensional 4^4 (brick-like) net (Figure 1 c).[14] Interpenetration of two such 4^4 nets leads to a $[Zn_2(bpdc)_2]$ layer. The bpee ligands coordinate to the Zn^{II}

---

[*] Dr. K. Li, H. Wu, Dr. D. H. Olson, Dr. T. J. Emge, W. Ki, Prof. Dr. J. Li
Department of Chemistry and Chemical Biology
Rutgers, The State University of New Jersey
Piscataway, NJ 08854 (USA)
Fax: (+1) 732-445-5312
E-mail: jingli@rutgers.edu

A. Lan, Dr. M. Hong
Fujian Institute of Research on the Structure of Matter
Chinese Academy of Sciences, Fuzhou (P.R. China)

[**] A.L. and K.L. contributed equally to this project. A.L. is currently a visiting scholar supported by the CAS/SAFEA International Partnership Program for Creative Research Teams for his research at Rutgers University. We are grateful for the financial support from the DOE (Grant No. DE-FG02-08ER46491).

Supporting information for this article is available on the WWW under http://dx.doi.org/10.1002/anie.200804853.

centers in two neighboring layers, completing the tetrahedral coordination sphere for each Zn^{II} center and connecting the layers into the overall 3D structure. It should be noted that all bpdc ligands within the layers, as well as the bpee ligands connecting the layers, are well separated. No significant π–π interactions occur within the framework (the closest carbon atoms within the π systems of bpdc and bpee are ca. 3.8 Å and 4.6 Å apart, respectively). Whereas the bpdc ligands are bent and twisted to accommodate the interpenetration, bpee ligands remain essentially co-planar.

The structure of **1** contains roughly rectangular 1D channels in which DMF solvent molecules are encapsulated, which can be removed either by heating under vacuum for an extended period of time or by evacuating at room temperature following solvent exchange with methanol and dichloromethane. Both treatments resulted in the same crystalline guest-free material. Guest-free **1** (referred to as **1′** hereafter) was confirmed by argon adsorption measurements to have a pore volume of 0.17 $cm^3 g^{-1}$, a narrow QSDFT (quenched solid density functional theory)[15] pore-size distribution around 7.5 Å and a Langmuir surface area of 483 $m^2 g^{-1}$ (see the Supporting Information). Removal of DMF led to distortion of the unit cell, as indicated by the shifts of the PXRD peaks. The distorted structure of **1′** can be reversed to the original structure by reintroducing DMF under mild conditions (see the Supporting Information). The measured amount of benzene adsorbed by a sample of **1′** matches well with the simulated benzene uptake (based on the framework structure of **1**), both corresponding to about eight benzene molecules per unit cell, which also suggests a facile transition between the two structures (see the Supporting Information). This type of guest-responsive change in MMOF structures has been well documented and considered as a beneficial feature for advanced applications.[12,16]

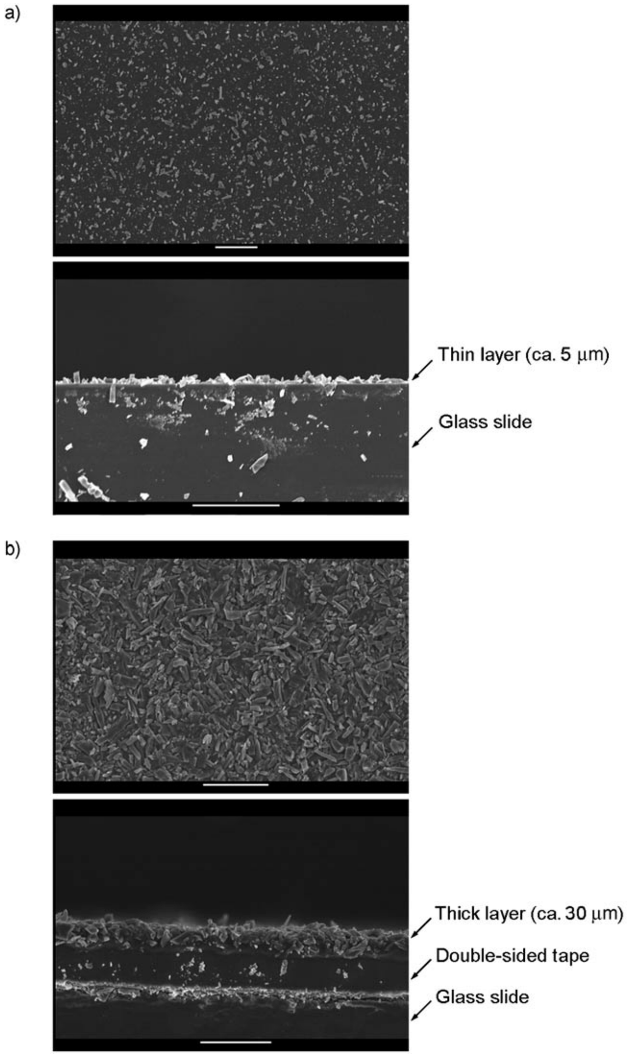

Figure 2. SEM images of typical thin (top two images) and thick (bottom two images) layers of 1′ crystals. Scale bars: 100 μm.

Framework **1′** is highly luminescent in the solid state at room temperature. H_2bpdc and bpee were chosen to build luminescent MMOFs targeted for sensing applications because their highly conjugated π-systems could act as both the sources of luminescence and the chemical recognition elements (binding sites). As expected, **1′** appears very bright to the eye when illuminated by a UV lamp (at 254, 304, and 350 nm). It was confirmed that the emission peak wavelengths and intensities are independent of the excitation wavelength between 260 nm and 340 nm, which can be explained by the broad and flat absorption bands and excitation spectra that cover the same region (see the Supporting Information). To demonstrate the applicability of **1′** for explosives detection, the fluorescence spectra of thin layers (ca. 5 μm, Figure 2, top) of **1′** were monitored, before and after exposing them to the equilibrated vapors of DNT (ca. 0.18 ppm at 25 °C) and DMNB (ca. 2.7 ppm at 25 °C) for varied periods of time (10 s, 30 s, 60 s, 90 s, 150 s, and 240 s, see the Supporting Information for the preparation of the layers). As shown in Figure 3, **1′** showed almost identically rapid and evident responses to both of the chemicals tested. Within ten seconds, the fluorescence quench percentages (defined as $(I_o - I)/I_o \times 100\,\%$; I_o = original peak maximum intensity, I = maximum intensity after exposure) reached almost the maxima for both DNT and DMNB (ca. 85 % and 84 %, respectively). No further quenching occurred with extended exposure. Whereas this degree of sensitivity to DNT vapor is comparable to that of the best performing conjugated polymer (CP) thin films, **1′** appears to respond to the quenchers more quickly and also outperforms CP thin films in its unprecedented high sensitivity towards DMNB in the vapor phase.[4,9] There are only two other materials reported so far that are able to detect DMNB vapors, exhibiting approximately 40 % (90 nm thick film, 10 s exposure; ca. 73 % quench at 2 min in a sealed cuvette)[17] and 20 % quench (film thickness unknown, 20 s exposure),[10] respectively. In addition, detections of both DNT and DMNB with **1′** are fully reversible. After quenching, the photoluminescence of **1′** can be recovered by simply heating the layer at 150 °C for about one minute (Figure 3 and Supporting Information). There are obvious red-shifts of the fluorescence peaks upon exposure to DNT and DMNB (Figure 3). Such a peak shifting also occurs with other analytes (see the Supporting Information), indicative of guest-dependent interactions between the MOF host framework and the analytes.

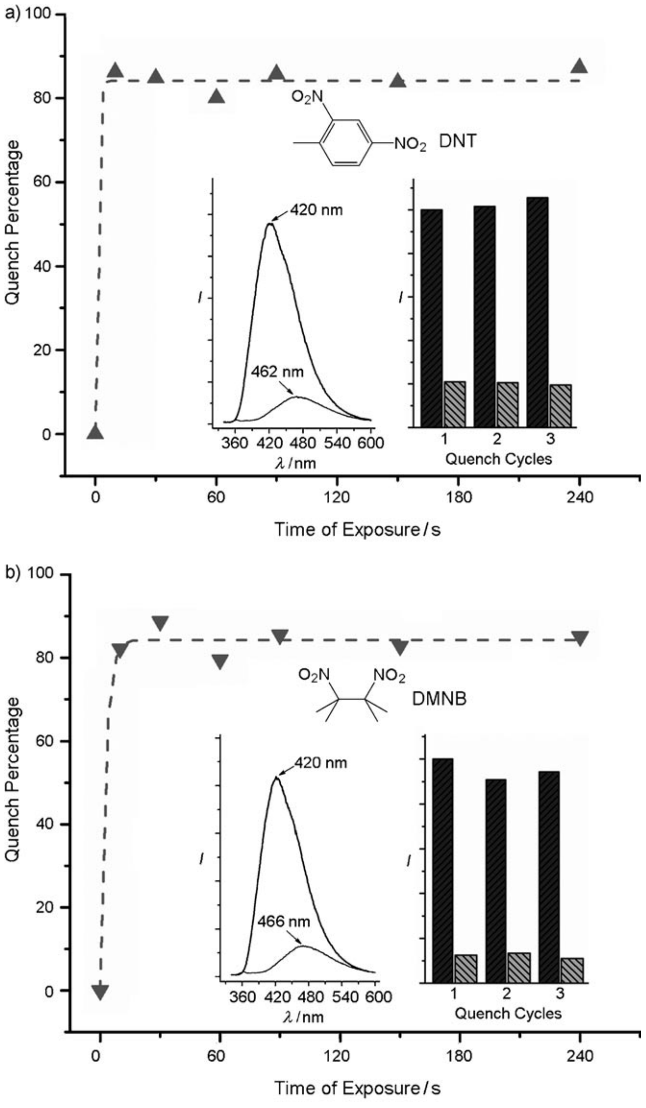

Figure 3. Time-dependent fluorescence quenching by a) 2,4-dinitrotoluene (DNT) and b) 2,3-dimethyl-2,3-dinitrobutane (DMNB; excitation wavelength = 320 nm). Insets: the corresponding fluorescence spectra before and after exposure to the analyte vapors for 10 s (left) and three consecutive quench/regeneration cycles (right).

The outstanding sensing capability of **1′** may be attributed to its infinite 3D framework structure and inherent microporosity. Studies of conjugated polymer thin films and other sensing materials have indicated that higher dimensionality enhances sensitivity because the excitons can be quenched by greater numbers of analyte binding sites through delocalization over the conjugated polymer backbone ("molecular wire" effect), through interchain energy migration in the solid state (films or aggregates), or through a highly organized molecular stacking structure.[4,17] Analogously, the extended three-dimensional network structure of **1′**, containing ordered π moieties, may also facilitate the migration of the excitons through similar mechanisms. The large optical band gap (ca. 3.1 eV) indicates that the framework in the excited state is highly reductive, providing an adequate driving force for the electron transfer to the DNT and DMNB quenchers.[10,17]

The effect of the microporosity in **1′** is twofold. Porous structure has been proven to be a favorable feature for the fast detection of explosive vapors by amplifying fluorescent polymer (AFP) films,[4] metalloporphyrin-doped mesostructured silica films,[9] and fluorescent nanofibril films.[8,17] The readily accessible micropores in **1′** and the fully exposed internal surface of a high Langmuir surface area of 483 $m^2\,g^{-1}$ provide facile diffusion routes and binding sites for the vapors, accounting for the very quick response times (ca. 10 s). Another evidence showing the importance of the microporosity is that thin layers of **1** (with pores occupied by DMF solvent molecules) showed dramatically lower responses to DMNB vapor (ca. 8 %). In this case, the quench occurs only at the external surfaces of the MOF, since the pores are already filled by DMF (Figure 4).

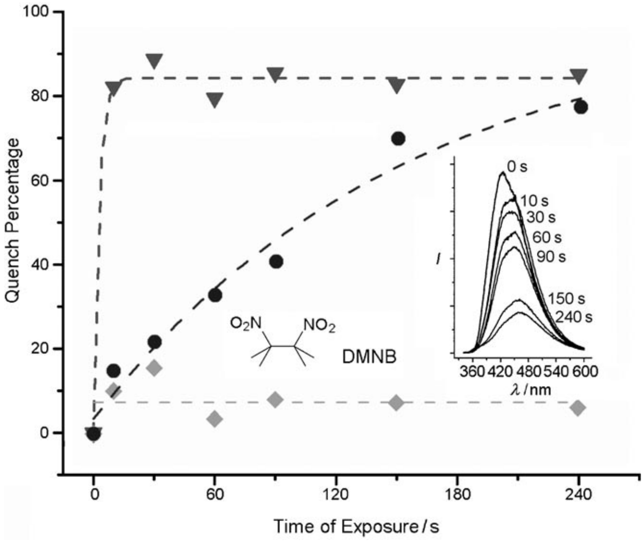

Figure 4. A comparison of the time-dependent fluorescence quenching by DMNB for thin layers of **1′** (▼), thick (dense) layers of **1′** (●), and thin layers of **1** (◆). Inset: the fluorescence spectra for a thick layer of **1′** at the specified exposure times.

As expected, thicker (and much denser) layers (ca. 30 μm, Figure 2) of **1′** showed slower fluorescence quenching responses, resulting from restricted diffusion. Similar dependence on film thickness was also detected in the CP films. However, the quench percentages for the thicker layers, given enough exposure time, approach the same level for the thin layers. This behavior is in contrast to the CP films, for which the quench efficiency normally plummets with increasing film thickness,[17] and also suggests that further reducing the size of the crystals of **1′** and the thickness of the layers should result in even faster responses but probably not higher sensitivity.

The excellent fluorescence quenching response to DMNB can be further attributed to the pore confinement of the analyte inside the molecular-sized cavities of **1′** which facilitates stronger interactions between the DMNB and the host framework, as is reflected by the relatively small difference in the quench percentages for nitrobenzene (NB), which exhibits only 10 % higher sensitivity (94 % quench at 10 s) compared to DMNB (see the Supporting

Information), despite drastic differences in their vapor pressures (ca. 300 ppm for NB compared with 2.7 ppm for DMNB at 25 °C) and reduction potentials (−1.15 V for NB compared with −1.7 V for DMNB), in addition to the flat structure of NB that favors a strong π–π interaction with the framework.[18] This effect may also account for the almost identical responses of **1′** to DNT and DMNB, although DNT has a more favorable reduction potential (−1.0 V vs. SCE) and π-type interactions.[18] A comparison of the quench response of **1′** with benzene (ca. 45 %, 1.3×10^5 ppm at 25 °C) and DMF (ca. 58 %, 1×10^4 ppm at 25 °C) vapors indeed suggests a degree of its selectivity towards different analyte species. Similar to the CPs, **1′** exhibits stronger responses to the more electron-deficient compounds (NB, DNT, and DMNB).

In summary, a highly luminescent MMOF, [Zn_2(bpdc)$_2$(bpee)], was designed and successfully synthesized. It is the first microporous crystalline metal–organic material able to detect trace explosives in the vapor phase, probably through a redox quenching mechanism similar to that in the conjugated polymer systems. Very fast responses and high sensitivity towards the representative nitroaromatic explosive, DNT, and the plastic explosive taggant, DMNB, were detected. The 84 % fluorescence quench efficiency by DMNB after merely ten second exposure is unprecedented. Furthermore, such detections were also proven to be reversible. These remarkable preliminary results point to a new and important application of microporous metal–organic framework materials. Comprehensive study of this material, as well as other luminescent MMOFs, is currently underway to fully understand the mechanism of their fluorescent quenching effect, and to further explore their potential in explosive sensing. It can be envisioned that one can develop a series of luminescent MMOFs (with different framework structures, band gaps, pore size/shape/nature, and etc.) that will have different responses towards the same analyte. By combining these MMOFs into a sensor array, finger-print like response pattern to each analyte may be attainable.[7,19] Considering the vast versatility of this type of materials, we anticipate that a fertile and exciting field toward developing highly sensitive and selective sensors or sensor arrays based on luminescent MMOFs will emerge.

Experimental Section

1′: A mixture of $Zn(NO_3)_2\cdot6H_2O$ (0.0892 g, 0.30 mmol), H_2bpdc (0.0727 g, 0.30 mmol) and bpee (0.0547 g, 0.30 mmol) in DMF (15 mL) was heated at 165 °C for 3 days to afford **1** as colorless block-shaped crystals (0.0817 g, 0.087 mmol, 58 %). A freshly made sample of **1** (0.0501 g, 0.053 mmol) was immersed in methanol (3 days) and dichloromethane (4 days) consecutively for solvent exchange, followed by removal of solvent under vacuum at room temperature to afford **1′** (0.0398 g, 0.050 mmol, 95 % yield).

2,4-dinitrotoluene (99 %) and 2,3-dimethyl-2,3-dinitrobutane (98 %) were purchased from TCI America and used as received. About 1 g of each were placed into two small open vials and the vials were placed into two capped bottles four days before the fluorescence quenching experiments to ensure equilibration of vapor pressures. The original fluorescence spectra of the layers (see the Supporting Information for preparation of the layers) were collected (the peak intensities of which were used to correct the effects of variations in layer thickness and morphology) before placing the layers into the bottles containing the analytes. At the specified exposure time, one layer was taken out and quickly mounted to the sample holder of a Varian Cary Eclipse fluorescence spectrophotometer and the fluorescence spectrum was collected without delay.

SEM images were taken on an Amray 1830 I scanning electron microscope (the samples were coated with a thin layer of gold–palladium beforehand for better contrast). Single crystal X-ray diffraction data of **1** were collected at 293(2) K on a Bruker-AXS smart APEX I CCD diffractometer with graphite-monochromated $Mo_{K\alpha}$ radiation ($\lambda = 0.71073$ Å). A total of 18781 reflections were collected (4349 unique, $R_{int} = 0.0474$) between a θ of 2° to 26.37°, The structure was solved by direct methods and refined by full-matrix least-squares on F^2 using the Bruker SHELXTL package. $R1 = 0.0447$ ($I > 2\sigma(I)$); $wR2 = 0.1047$ (all data); GoF = 1.007 (all data). Crystal data for **1**: $C_{46}H_{40}N_4O_{10}Zn_2$, $M_w = 939.56$ g mol^{-1}; monoclinic; space group $C2/c$; $a = 26.138(2)$, $b = 6.7464(4)$, $c = 25.024(2)$ Å; $\beta = 105.916(1)°$; $V = 4243.4(4)$ Å^3; $Z = 4$; $\rho_{calcd} = 1.471$ g cm^{-3}. CCDC 704475 contains the supplementary crystallographic data for this paper. These data can be obtained free of charge from The Cambridge Crystallographic Data Centre via www.ccdc.cam.ac.uk/data_request/cif.

Received: October 4, 2008
Revised: November 11, 2008

Keywords: explosives · fluorescence · metal–organic frameworks · microporous materials · sensors

---

[1] J. I. Steinfeld, J. Wormhoudt, *Annu. Rev. Phys. Chem.* **1998**, *49*, 203.
[2] K. G. Furton, L. J. Myers, *Talanta* **2001**, *54*, 487.
[3] P. Kolla, *Angew. Chem.* **1997**, *109*, 828–839; *Angew. Chem. Int. Ed. Engl.* **1997**, *36*, 800; A. G. Davies, A. D. Burnett, W. H. Fan, E. H. Linfield, J. E. Cunningham, *Mater. Today* **2008**, *11*, 18.
[4] S. W. Thomas III, G. D. Joly, T. M. Swager, *Chem. Rev.* **2007**, *107*, 1339.
[5] S. J. Toal, W. C. Trogler, *J. Mater. Chem.* **2006**, *16*, 2871.
[6] L. Senesac, T. G. Thundat, *Mater. Today* **2008**, *11*, 28; R. Y. Tu, B. H. Liu, Z. Y. Wang, D. M. Gao, F. Wang, Q. L. Fang, Z. P. Zhang, *Anal. Chem.* **2008**, *80*, 3458; T. L. Andrew, T. M. Swager, *J. Am. Chem. Soc.* **2007**, *129*, 7254; H. Sohn, M. J. Sailor, D. Magde, W. C. Trogler, *J. Am. Chem. Soc.* **2003**, *125*, 3821.
[7] M. E. Germain, M. J. Knapp, *J. Am. Chem. Soc.* **2008**, *130*, 5422.
[8] T. Naddo, Y. K. Che, W. Zhang, K. Balakrishnan, X. M. Yang, M. Yen, J. C. Zhao, J. S. Moore, L. Zang, *J. Am. Chem. Soc.* **2007**, *129*, 6978.
[9] S. Y. Tao, G. T. Li, H. S. Zhu, *J. Mater. Chem.* **2006**, *16*, 4521.
[10] S. W. Thomas III, J. P. Amara, R. E. Bjork, T. M. Swager, *Chem. Commun.* **2005**, 4572.
[11] G. Férey, *Chem. Soc. Rev.* **2008**, *37*, 191; M. Vallet-Regí, F. Balas, D. Arcos, *Angew. Chem.* **2007**, *119*, 7692; *Angew. Chem. Int. Ed.* **2007**, *46*, 7548; S. Kitagawa, R. Kitaura, S.-I. Noro, *Angew. Chem.* **2004**, *116*, 2388; *Angew. Chem. Int. Ed.* **2004**, *43*, 2334; D. Maspoch, D. Ruiz-Molina, J. Veciana, *Chem. Soc. Rev.* **2007**, *36*, 770; O. M. Yaghi, *Nat. Mater.* **2007**, *6*, 92; J. Y. Lee, D. H. Olson, L. Pan, T. J. Emge, J. Li, *Adv. Funct. Mater.* **2007**, *17*, 1255; L. Pan, B. Parker, X. Y. Huang, D. H. Olson, J. Lee, J. Li, *J. Am. Chem. Soc.* **2006**, *128*, 4180; L. Pan, D. H. Olson, L. R. Ciemnolonski, R. Heddy, J. Li, *Angew. Chem.* **2006**, *118*, 632; *Angew. Chem. Int. Ed.* **2006**, *45*, 616; L. Pan, H. Liu, X. Lei, X. Huang, D. H. Olson, N. J. Turro, J. Li, *Angew. Chem.* **2003**, *115*, 560; *Angew. Chem. Int. Ed.* **2003**, *42*, 542; L. Pan, H. Liu, S. P. Kelly, X. Huang, D. H. Olson, J. Li, *Chem. Commun.* **2003**, 854;

K. Li, D. H. Olson, J. Lee, W. Bi, K. Wu, T. Yuen, Q. Xu, J. Li, *Adv. Funct. Mater.* **2008**, *18*, 2205.

[12] C. A. Bauer, T. V. Timofeeva, T. B. Settersten, B. D. Patterson, V. H. Liu, B. A. Simmons, M. D. Allendorf, *J. Am. Chem. Soc.* **2007**, *129*, 7136.

[13] B. Chen, Y. Yang, F. Zapata, G. Lin, G. Qian, E. B. Lobkovsky, *Adv. Mater.* **2007**, *19*, 1693; K. L. Wong, G. L. Law, Y. Y. Yang, W. T. Wong, *Adv. Mater.* **2006**, *18*, 1051; D. Tanaka, S. Horike, S. Kitagawa, M. Ohba, M. Hasegawa, Y. Ozawa, K. Toriumi, *Chem. Commun.* **2007**, 3142; C. Serre, F. Pelle, N. Gardant, G. Ferey, *Chem. Mater.* **2004**, *16*, 1177.

[14] A. F. Wells, *Three-dimensional Nets and Polyhedra*, Wiley, New York, **1977**.

[15] P. I. Ravikovitch, A. V. Neimark, *Langmuir* **2006**, *22*, 11171.

[16] T. K. Maji, R. Matsuda, S. Kitagawa, *Nat. Mater.* **2007**, *6*, 142; D. Tanaka, K. Nakagawa, M. Higuchi, S. Horike, Y. Kubota, T. C. Kobayashi, M. Takata, S. Kitagawa, *Angew. Chem.* **2008**, *120*, 3978; *Angew. Chem. Int. Ed.* **2008**, *47*, 3914; N. Yanai, W. Kaneko, K. Yoneda, M. Ohba, S. Kitagawa, *J. Am. Chem. Soc.* **2007**, *129*, 3496; T. K. Maji, S. Kitagawa, *Pure Appl. Chem.* **2007**, *79*, 2155.

[17] T. Naddo, X. Yang, J. S. Moore, L. Zang, *Sens. Actuators B* **2008**, *134*, 287.

[18] J.-S. Yang, T. M. Swager, *J. Am. Chem. Soc.* **1998**, *120*, 11864; J.-S. Yang, T. M. Swager, *J. Am. Chem. Soc.* **1998**, *120*, 5321.

[19] K. J. Albert, N. S. Lewis, C. L. Schauer, G. A. Sotzing, S. E. Stitzel, T. P. Vaid, D. R. Walt, *Chem. Rev.* **2000**, *100*, 2595.